PROTON-IRRADIATION INDUCED CHEMICAL ORDERING OF FePt NANOPARTICLES

Naidu V. Seetala[1*], J. W. Harrell[2], Zhiyong Jia[2], David E. Nikles[2], Gary A. Glass[3], and Bibhudutta Rout[3]

[(1)] Department of Physics, RWE Jones Drive, Carver Hall 81, Grambling State University, Grambling, LA 71245
[*] Corresponding author, email: naidusv@gram.edu
[(2)] MINT Center, University of Alabama, Tuscaloosa, AL 35487
[(3)] Louisiana Accelerator Center, University of Louisiana at Lafayette, Lafayette, LA 70504

High temperature (> 500 °C) annealing of FePt nanoparticles to obtain the desired high-anisotropy $L1_0$ phase for magnetic storage media is a problem due to particle sintering. In order to reduce the phase transformation temperature and minimize sintering, we previously (Ref. 1) used 300 keV Al^+-irradiation and observed partial ordering at ~ 220 °C, but further annealing showed detrimental effects due to lattice strain produced by defect clusters. Here, we used 1 MeV proton-irradiation at < 100 °C to a dose of 5 x 10^{16} ions/cm^2 with current density ~ 0.15 nA/cm^2 to minimize the formation of vacancy clusters during post-irradiation annealing. The vacancy concentration estimated from SRIM-2006 code is about three orders of magnitude less in proton-irradiation compared to Al^+-ion irradiation. Although the magnetization results show that the chemical ordering starts at ~ 200 °C in proton-irradiated FePt nanoparticles, it is less prominent compared to Al^+-ion irradiation; and the detrimental effects of vacancy clusters seem to remain stronger even at higher temperatures. The differences in the collision cascades and Frankel pair recombination may explain these discrepancies.

I. INTRODUCTION

FePt nanoparticles are excellent candidates for magnetic storage media. The $L1_0$ phase of FePt has a very high value of magnetocrystalline anisotropy density (K_u ~ 7 x 10^7 erg/cc) (Ref. 2-3), and particles as small as 4 nm in diameter are observed to have a thermal stability factor (K_uV/kT) of 57. This thermal stability would be adequate for magnetic storage media applications. A team from IBM[4] first reported the chemical synthesis of 4 nm diameter FePt nanoparticles with a narrow size distribution. Self-assembly of these particles could yield a magnetic storage density in the terabit per square inch (Tbit/in^2) range. Chemically synthesized FePt particles usually are in the FCC phase and they need to be thermally annealed above 500 °C to transform to the $L1_0$ phase with high magnetic anisotropy and large magnetic coercivity. The main problem with annealing is the particle aggregation and sintering. The self-assembly of the particles is also disturbed as the surfactants used in the self-assembly decompose at these high annealing temperatures. In order to overcome these problems, several techniques have been attempted: 1) Direct synthesis of nanoparticles at high temperatures[5], 2) Using additives such as Au and Ag during the particle synthesis to lower the transition temperature[6-8], 3) High temperature solution annealing of nanoparticles prior to the self-assembly[5], and 4) Heavy-ion irradiation of self-assembled particles[1].

Ion-irradiation produces lattice defects (vacancies). Their migration at low temperatures assists the phase transformation. Post-deposition He^+-beam irradiation of FePt sputtered films[9] and Ar^+-irradiation of Fe/Pt multi layers[10] allowed chemical ordering at low temperatures induced by radiation defects. Lowering of the $L1_0$ ordering temperature by more than 100 °C of isolated FePt nanoparticles by He^+-ion irradiation has been reported recently[11]. We have achieved[1] a partial chemical ordering in 300 keV Al^+-irradiated 4-5 nm self-assembled FePt and FePt(14%Au) nanoparticles at post-irradiation annealing temperatures as low as 220 °C. The vacancy defects produced during ion-irradiation and their mobility during subsequent annealing enhanced the bulk diffusion that resulted in higher magnetic anisotropy. But, further annealing at higher temperatures showed detrimental effects due to larger vacancy cluster formation and its stress on the lattice structure. Here, we tried to use proton-irradiation to minimize the detrimental effects due to larger vacancy cluster formation upon further annealing.

II. EXPERIMENTAL

The FePt nanoparticles with narrow size distribution (~ 5 nm $\pm$ 5%) were prepared using a method similar to that reported by the IBM group[12]. The particles synthesis

involves simultaneous polyol reduction of platinum acetylacetonate and iron chloride in the presence of organic surfactants. A solution of platinum acetylacetonate (0.5 mmol), iron chloride (0.7 mmol), and 1,2-hexadecanediol (2 mmol) in 25 mL Phenyl ether was heated to 100 °C in a three-necked round-bottom flask under a nitrogen atmosphere for 10 min. Oleic acid (0.5 mmol) and oleylamine (0.5 mmol) were added, and the mixture was heated to 200 °C for 20 min. $Li(et)_3BH$ (1M THF solution) was slowly dropped into the mixture over 2 min. The black dispersion was stirred at 200 °C for 5 min under N_2 and refluxed at 263 °C for 30 min. The heat source was removed and the dispersion was allowed to cool to room temperature. The particles were dispersed in 1 mL hexane containing 0.1 mL of 50/50 oleylamine and oleic acid. Depositing the dispersions onto a silicon wafer and slowly evaporating gave self-assembled FePt nanoparticle films with FePt nanoparticles in a close-packed lattice.

The proton-irradiation of these films was performed at Louisiana Accelerator Center, UL-Lafayette using a NEC 5SDH-2 1.7 MV tandem Pelletron accelerator with 1 MeV H^+-ions to a dose 5 x 10^{16} ions/cm^2 at < 100 °C and current density of 0.15 nA/cm^2. The irradiation temperature is maintained to be low such that the irradiation-induced vacancies do not form vacancy clusters such as voids. In case of 300 keV Al^+-ion irradiation the beam current was high, thus the samples were held down with Ti clips to a water-cooled thin Ti plate to maintain the low irradiation temperature, which was measured by an optical pyrometer to be around 43 °C. The irradiation temperature for the proton-irradiated sample is not directly measured, but from our previous experience and the current density used, we estimated it to be < 100 °C. The ion irradiation conditions for Al^+-ions and protons are compared in Table I. A computer simulation code SRIM-2006 (Ref. 13) is used to estimate the depth profile, the energy loss, and the defect creation in the FePt nanoparticles.

TABLE I. Comparison of Ion-irradiation Conditions

Parameter	**Al^+-ions**	**H^+-ions**
Ion energy	300 keV	1 MeV
Irradiation temperature (°C)	43	< 100
Beam current (nA/cm^2)	98.4	0.15
Total dose (ions/cm^2)	1 x 10^{16}	5 x 10^{16}

Post-irradiation annealing was performed in a Lindberg tube furnace for 60 minutes at each desired temperature, with Ar_2 (5% H_2) flow. Magnetic studies were carried out at room temperature using a Princeton Measurements Model 2900 Alternating Gradient Magnetometer with maximum applied field of 19 kOe.

III. RESULTS AND DISCUSSION

III.A. SRIM Analysis of Ion-Irradiation

The SRIM-2006 computer simulation is run for one million ions into a 5 nm FePt target. A density value of 14 g/cm^3 is used for FePt nanoparticles. FePt bulk density is close to 15 g/cm^3. Since the mass density within the surface region of the nanoparticles is different from that in the interior, an estimate of 14 g/cm^3 is made[14] for the FePt nanoparticles density assuming ~ 4% surface lattice constant change for the surface layers. The ion trajectories are displayed in Fig. 1 for 300 keV Al^+-ions and 1 MeV protons in 5 nm FePt. The lateral distribution is much larger for Al^+-ions compared to that for protons. Similar depth profiles distributions (not shown) are observed for Fe and Pt recoil atoms (i.e. much wider distribution in Al^+-irradiation and very narrow distribution in proton-irradiation). This may result in more uniform defect distribution in Al^+-irradiated samples compared to the proton-irradiated samples.

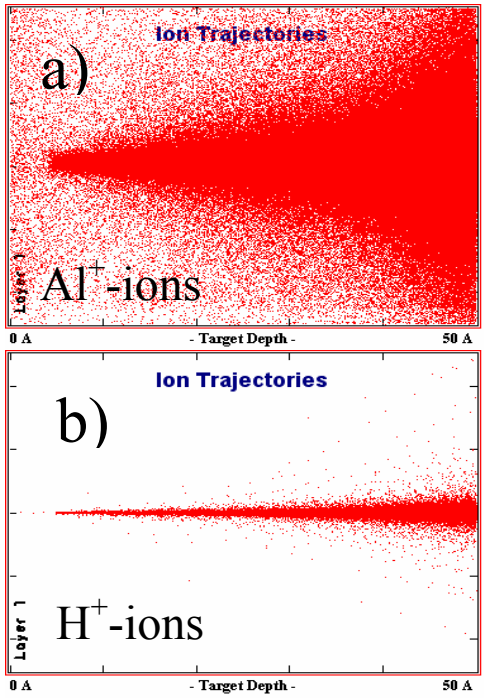

Fig. 1. Ion Trajectories in 5 nm FePt for a) 300 keV Al^+-ions and b) 1MeV protons (with 1 million ions in each case for SRIM calculations).

The SRIM estimates of energy loss and defect concentrations are compared in Table II for 300 keV Al^+- and 1MeV H^+-irradiation in 5 nm FePt particles. The electronic stopping powers are not that different for both Al^+-ions and protons, but the nuclear stopping power for Al^+-ions is several orders of magnitude higher compared to protons. The energy transferred to Fe and Pt recoils by

the ions is also remarkably different, about three orders of magnitude higher for Al^+-ions compared to protons. This results in smaller size cascades and low damage in proton-irradiation.

TABLE II. SRIM-2006 Estimates for Energy Transfer and Defect Production in 5 nm FePt Nanoparticles Irradiated by 300 keV Al^+-ions and 1 MeV Protons.

Parameter	300 keV Al^+	1 MeV H^+
Range in FePt (μm)	0.15	6.1
Stopping Power (electronic) (eV/Å)	75	11.2
Stopping Power (nuclear) (eV/ Å)	36	0.01
Energy to Fe (eV/ion over 5 nm)	733	0.1
Energy to Pt (eV/ion over 5 nm)	1770	0.2
Fe-replacements/ Å /ion	39	0.013
Pt-replacements/ Å /ion	2.2	0.001
Dose (ions/cm^2)	1 x 10^{16}	5 x 10^{16}
Vacancies (cm^{-3})	4 x 10^{22}	6.5 x 10^{19}

The estimated range of 300 keV Al^+-ions in FePt and 1 MeV protons are 0.15 and 6.1 μm, respectively. These are many times the size of FePt nanoparticles. Thus the ions completely pass through, producing a high density of lattice defects (vacancies and interstitials) in the nanoparticles. TRIM[15] simulations are used to estimate the number of vacancies produced. Due to recombination during irradiation, only 10% of the vacancies are expected to remain[16]. The vacancy concentration (Table II) is three orders of magnitude less in proton-irradiation compared to Al^+-irradiation, thus we expect less vacancy cluster formation during post-irradiation annealing for proton-irradiated samples.

In the previous studies the FePt sputtered films were heated during irradiation in order to enhance vacancy migration and chemical ordering. But in our case we maintained the irradiation temperature (< 100 °C) below the vacancy migration temperature (vacancies migrate at above 180 °C) in order to retain the vacancies to study their effects during post-irradiation annealing. Due to the high rate of defect production and energy dissipation in the case of Al^+-irradiation, it was necessary to cool the target. The target was water-cooled to maintain the temperature at ~ 43 °C.

III.B. Magnetic Characteristics of Ion-irradiated FePt

The hysteresis curves for the irradiated samples, as-irradiated and at the post-irradiation temperature where highest coercivity H_c is observed are shown in Fig. 2. The as-irradiated samples showed partial chemical ordering with H_c ~ 127 Oe for Al^+-irradiated and 280 Oe for 1 MeV proton-irradiated FePt nanoparticles. Although the irradiation produced vacancy concentration is lower for protons, it gave higher H_c, which may be explained by higher irradiation temperature during proton-irradiation or variations in the starting batch of FePt particles.

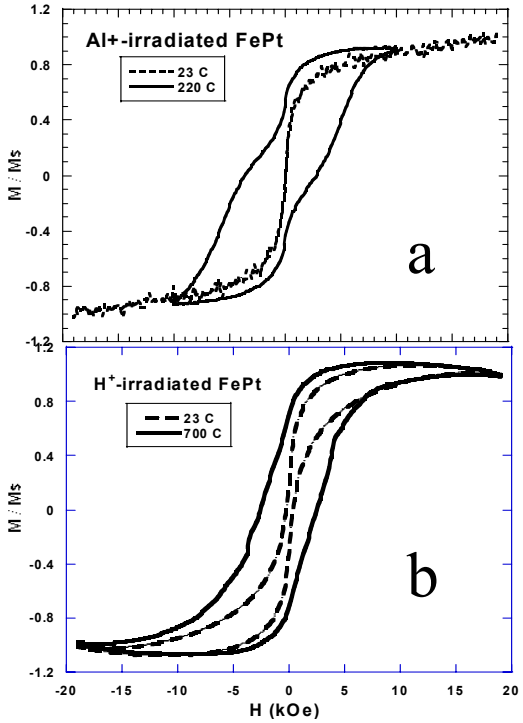

Fig. 2. Hysteresis curves for as-irradiated (dashed lines) and post-irradiation annealed (solid lines) FePt nanoparticles for a) 300 keV Al^+-ions and b) 1 MeV proton-irradiated samples.

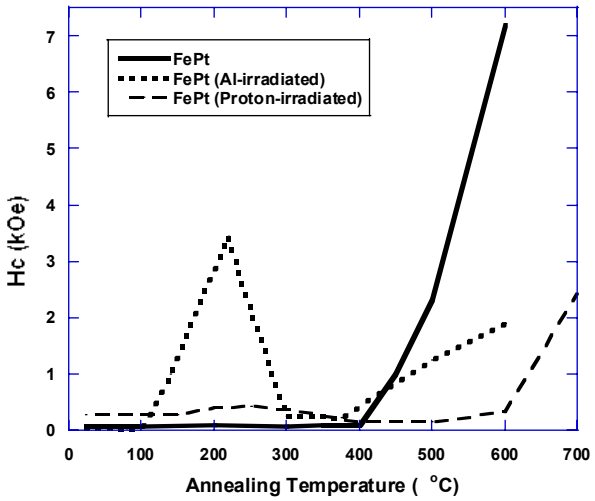

Fig. 3. Variations in Coercivity H_c with annealing temperature for a) un-irradiated, b) Al^+-ion irradiated, and c) proton-irradiated FePt nanoparticles.

The variations in coercivity with annealing temperature are shown in Fig. 3 for un-irradiated FePt, Al^+-irradiated, and proton-irradiated FePt nanoparticles. The curves show that the $L1_0$ chemical ordering occurs only above 450 °C in FePt nanoparticles, whereas it stars at ~ 200 °C in proton- or Al^+-irradiated FePt nanoparticles. The increase in H_c is very small in proton-irradiated FePt, which may be understood in terms of lower vacancy production (Table II). But the detrimental effects[1] of larger vacancy clusters and their stress on the lattice structure seems to remain stronger even at higher temperatures in proton-irradiated samples indicated by the variations in H_c with annealing temperature and the DCD curves (see discussion on Fig. 5).

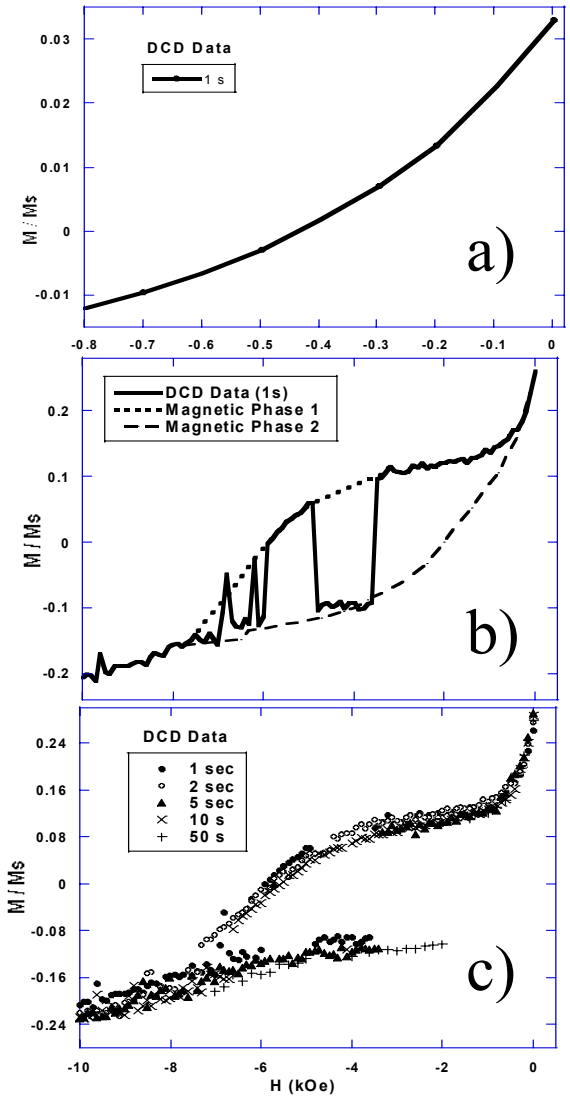

Fig. 4. DC demagnetization time dependent remanent curves for FePt nanoparticles: a) un-irradiated, b) Al^+-irradiated and annealed at 300 °C, showing fluctuations between two magnetic phases, and c) same as 'b' run with different wait times at the reverse field.

The DC demagnetization time dependent remanent curves of the irradiated samples exhibited an unusual behavior during post-irradiation annealing that may be associated with lattice strain produced by larger defect clusters formed during annealing[1]. Fig. 4 shows switching between two magnetic phases in DC demagnetization remanent curves for the Al^+-irradiated FePt nanoparticles post-annealed at 300 °C, whereas the un-irradiated sample showed a smooth curve with a single phase (note the x-axis scale for un-irradiated sample Fig. 4a is different from irradiated sample Fig 4b&c, as the as-made FePt has very low remanent coercivity). The two-phase fluctuations may be related to pinning and thermally activated de-pinning of the magnetization at the vacancy cluster sites. Similar behavior is observed in proton-irradiated FePt nanoparticles.

Fig. 5 shows the DCD time dependent remanent curves for proton-irradiated FePt nanoparticles post-irradiation annealed at different temperatures. Interestingly, the switching from the normal (hard) state to the defect (soft) state moves to lower applied magnetic reversal field with the increasing wait time at the reversal field. Usually a single step switching is observed in proton-irradiated FePt nanoparticles, while multiple switching (back and forth) between the two phases is observed in the Al^+-irradiated FePt nanoparticles. This indicates that the lattice strain created by the vacancy clusters in the Al^+-irradiated FePt is weaker to a level where the thermal energy fluctuations is enough to make the multiple switching possible. This suggests that the vacancy clusters in proton-irradiated FePt may be larger than that in Al^+-irradiated FePt. It is puzzling since the SRIM analysis gave three orders of magnitude fewer vacancies in proton-irradiated particles compared to that in Al^+-irradiated particles. It may be possible to understand these discrepancies by considering the size of the cascades and the thermal spikes with in the cascades in these two irradiation conditions. The lateral distribution of ion and recoil trajectories described above (Fig. 1) may indicate the probability of vacancies within close vicinity of interstitials is high for Al^+-irradiation. This gives more Frankel pair recombination resulting in smaller vacancy clusters for Al^+-irradiation. On the other hand, proton trajectories showed narrow lateral distribution that could result in non-uniform distribution of vacancies and interstitials thus less number of Frankel pairs for recombination. There is also higher probability of diffusion of the isolated interstitials to particle surfaces as the interstitial diffusion is found to be higher for nanoparticles compared to the bulk. In addition, the probability of pair recombination during irradiation is less for proton-irradiation since the energy transferred to Fe and Pt recoils by the protons is several orders of magnitude lower compared to Al^+-ions that results in smaller cascades and weaker thermal spikes.

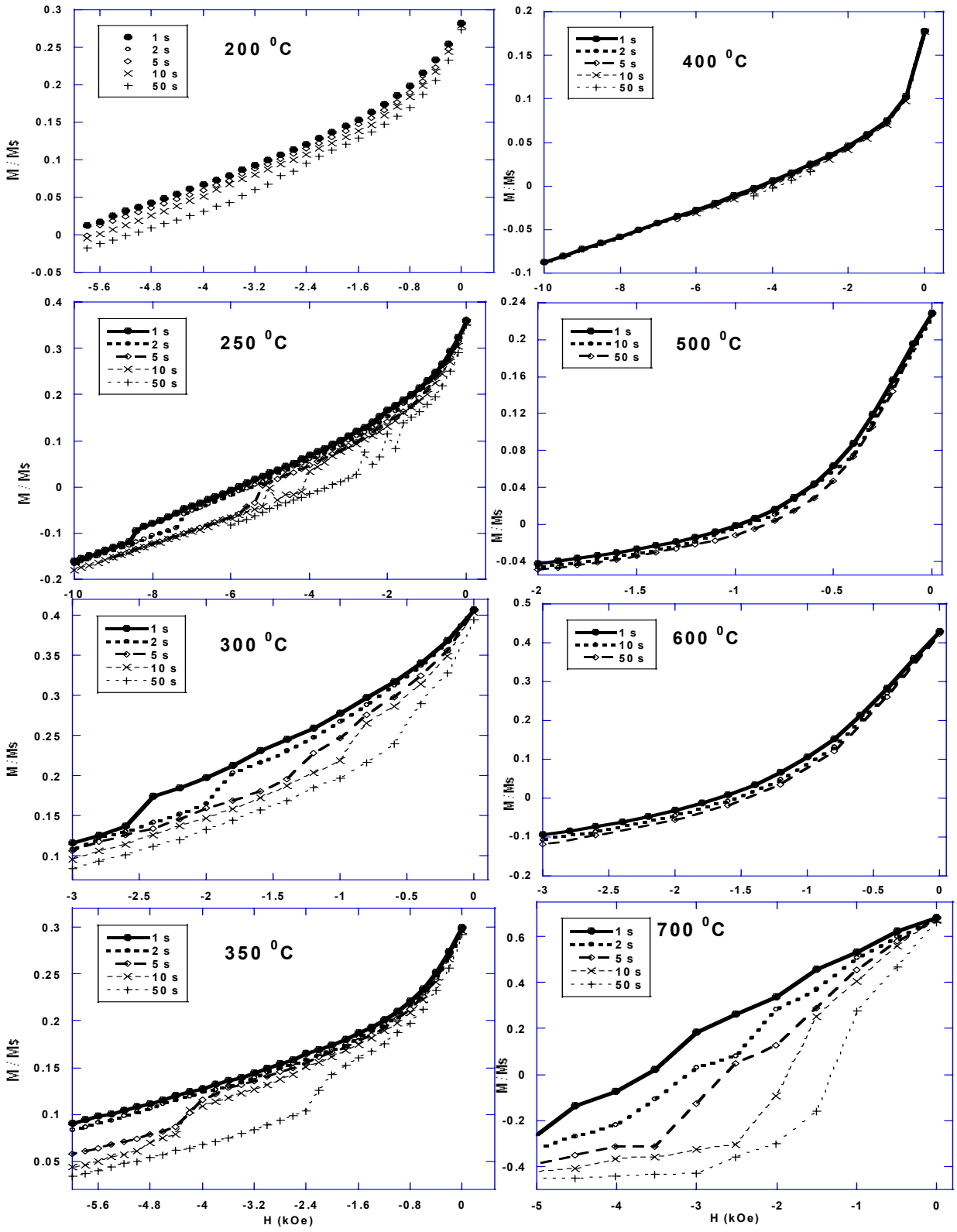

Fig. 5. DC demagnetization time dependent remanent curves for proton-irradiated FePt nanoparticles post-irradiation annealed at different temperatures.

Another point to note in Fig. 5 is the variation in the intensity of switching between the two phases, i.e. the step size, with the post-irradiation annealing temperature. The intensity of the switching has increased with the annealing temperature up to 350 °C and then decreased till 700 °C, where the reappearance of larger steps is observed. These variations correlate with the H_c dependence with temperature seen in Fig. 3. This indicates vacancies migrate during post-irradiation annealing forming larger size vacancy clusters, resulting in a higher lattice strain that results in lowering the coercivity (see Fig. 3). At around 700 °C, the vacancy clusters (voids) dissociate and that resulted in a sharp increase in H_c at 700 °C as the lattice strain is relieved. Dissociation of voids at these high temperatures in irradiated metals is well known[17, 18].

The remanent coercivity of randomly oriented nanoparticles is often approximated by the Sharrock formula[19], which is given by

$$H_{cr} = H_0 \left\{ 1 - \left[\frac{k_B T}{K_u V} \ln(f_0 t) \right]^{2/3} \right\}, \qquad (1)$$

where H_0 is the intrinsic (short time) coercivity, K_u is the uniaxial anisotropy energy, V is the particle switching volume, k_B is the Boltzmann constant, T is absolute temperature, f_0 is the attempt frequency (~10^9-10^{10} Hz), and t is the wait time at reverse field[20]. The time dependent remanent coercivity as a function of annealing temperature is fitted to the Sharrock formula to determine H_0 and the thermal stability factor, K_uV/k_BT. Using the thermal stability factor[5] we derived the values for K_u.

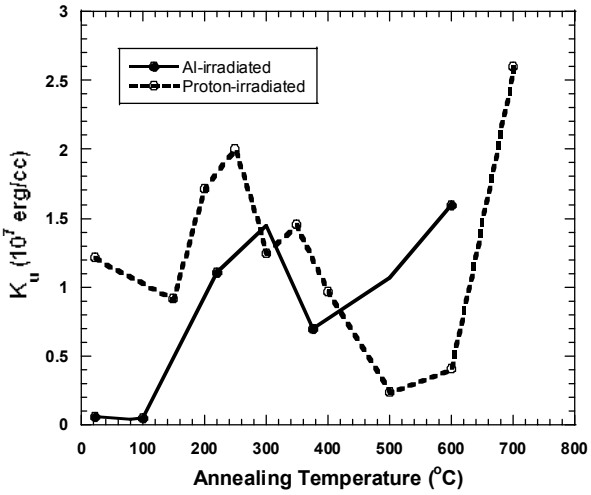

Fig. 6. Variations in magnetic anisotropy energy constant K_u with post-irradiation annealing of 300 keV Al^+-ions irradiated (solid line) and proton-irradiated (dotted line) FePt nanoparticles.

K_u is expected to increase with the degree of chemical ordering. Fig. 6 shows higher K_u values for proton-irradiated samples till about 400 °C indicating a higher degree of chemical ordering. But the H_c values shown in Fig. 3 are lower for the proton-irradiated sample in this temperature region. This may be explained by a wider particle size distribution for FePt nanoparticles used in proton-irradiation, which is also supported by the nature of the hysteresis curve shown in Fig. 2b (dashed line) that is wider at moderate applied magnetic fields and narrows down as the field is decreased. However, the K_u values above 200 °C are $\geq 1 \times 10^7$ erg/cc with a dip at ~ 500 °C for proton-irradiated sample. These values indicate that a significant chemical ordering is possible by ion-irradiation.

IV. CONCLUSIONS

Both, 300 keV Al^+-irradiation and 1 MeV proton-irradiation at < 100 °C in ~ 5 nm FePt nanoparticle induced partial chemical ordering indicated by an increase in magnetic coercivity H_c and uniaxial anisotropy energy density K_u values in the order of 10^7 erg/cc. Post-irradiation annealing initially increased H_c and K_u starting at ~ 200 °C; the values decreased upon further annealing at higher temperatures. This behavior is assigned to the irradiation induced vacancy migration that initially enhanced chemical ordering and at higher temperatures it decreased due to vacancy clusters formation that created a lattice strain in the nanoparticles. This detrimental effect is observed to be stronger in proton-irradiated FePt nanoparticles and continued to higher temperatures, although the SRIM estimated irradiation induced vacancies are three orders of magnitude lower in proton-irradiation compared to the Al^+-ion irradiation.

We tried to understand the discrepancies in terms of the differences in magnitude of cascades, thermal spikes within cascades, and Frankel pair recombination between the two irradiations. Anomalous features are observed in DC demagnetization time dependent magnetic reversal curves that correlates with the idea of lattice strain created by vacancy cluster formation during annealing and their dissociation at around 700 °C.

ACKNOWLEDGMENTS

This work has been partly supported by the NSF Materials Research Science and Engineering Center (MRSEC) award number DMR-0213985.

REFERENCES

1. N. V. Seetala, J. W. Harrell, J. Lawson, D. E. Nikles, J. R. Williams, and T. Isaacs-Smith, "Ion-irradiation Induced Chemical Ordering of FePt and FePtAu Nanoparticles**",** *Nucl. Inst. & Methods* **B241**, 583 (2005).
2. D. Weller and A. Moser, "Thermal Effect Lmits in Ultra-high Density Magnetic Recording" *IEEE Trans. Magnetics* **35**, 4423 (1999).
3. D. Weller, A. Moser, L. Folks, M. E. Best, L. Wen, M. F. Toney, M. Schwickert, J. U. Thiele, and M.F. Doerner, "High K_u Materials Approach to 100 Gbits/in^2," *IEEE Trans. Magn.* **36**, 10 (2000).
4. S. Sun, C. B. Murray, D. Weller, L. Folks, and A. Moser, "Monodisperse FePt Nanoparticles and Ferromagnetic FePt Nanocrystal Superlattices," *Science* **287**, 1989 (2000).
5. J. W. Harrell, D. E. Nikles, S. S. Kang, X. C. Sun, Z. Jia, S. Shi, J. Lawson, G. B. Thompson, and C. Srivastava, "Effect of Metal Additives on $L1_0$ Ordering of Chemically Synthesized FePt Nanoparticles," *Scripta Materialia* **53,** 411 (2005).
6. S. Kang, D. E. Nikles, and J. W. Harrell, "Reduction of Ordering Temperature of Self-assembled FePt Nanoparticles by the Addition of Ag", *Nano Letters* **2**, 1033 (2002).
7. S. Kang, D. E. Nikles, and J. W. Harrell, "Synthesis, chemical ordering and magnetic properties of FePt-Ag nanoparticles", *J. Appl. Phys*. **93**, 7178 (2003).
8. S. Kang, Z. Jia, D. E. Nikles, and J. W. Harrell, "Synthesis, Self-assembly and Magnetic Properties of $[FePt]_{1-x}Au_x$ Nanoparticles", *IEEE Trans. Magnetics* **39**, 2753 (2003).
9. H. Bernas, J. P. Attane, K. H. Heinig, D. Halley, D. Ravelosona, A. Marty, P. Auric, C. Chappert, and Y. Samson, "Ordering Intermetallic Alloys by Ion Irradiation: A Way to Tailor Magnetic Media", *Phys. Rev. Lett.* **91**, 77203-1 (2003).
10. V. R. Reddy, S. Kavita, S. Amirthapandian, A. Gupta, and B. K. Panigrahi, "Study of Low Energy Ar^+-ion Irradiated Fe/Pt Multilayers", *J. Phys.: Condens. Matter* **18**, 6401 (2006).
11. U. Wiedwald, A. Klimmer, B. Kern, L. Han, H. G. Boyen, P. Ziemann, and K. Fauth, "Lowering of the $L1_0$ Ordering Temperature of FePt Nanoparticles by He^+-ion Irradiation", *Appl. Phys. Lett*. **90**, 62508 (2007).
12. S. Sun, S. Anders, T. Thomson, J. E. E. Baglin, M. F. Toney, H. F. Hamann, C. B. Murray, and B. D. Terris, "Controlled Synthesis and Assembly of FePt Nanoparticles", *J. Phys. Chem*. **B107**, 5419 (2003).
13. J. F. Ziegler and J. P. Biersak, http://www.srim.org/.
14. X. W. Wu, C. Liu, L. Li, P. Jones, R. W. Chantrell, and D. Weller, "Nonmagnetic Shell in Surfactant-Coated FePt Nanoparticles", *J. Appl. Phys*. **95**, 6810 (2004).
15. J. F. Ziegler, J. P. Biersak, and U. Littmark, 'The Stopping of Ions in Matter', Pergamon, New York, 1985.
16. D. Ravelosona, C. Chappet, V. Mathet, and H. Bernas, "Chemical Order Induced by Ion-irradiation in FePt (001) Films", *Appl. Phys. Lett*. **76**, 236 (2000).
17. S. V. Naidu, A. Sen Gupta, and P. Sen, "Positron Annihilation Studies on Alpha-irradiated and Deformed Niobium", *J. Nucl. Mat*. **148**, 86 (1987).
18. S. V. Naidu, A. Sen Gupta, R. K. Bhandari, and P. Sen, "Defect Studies in Alpha-irradiated and Deformed Niobium by positron annihilation", Solid State Comm. **55**, 27 (1985).
19. M. P. Sharrock, "Time Dependence of Switching Fields in Magnetic Recording Media", *J. Appl. Phys*. **76**, 6413 (1994).
20. Y. K. Takahashi, T. Koyama, M. Ohnuma, T. Ohkubo, and K. Hono, "Size Dependence of Ordering in FePt Nanoparticles", *J. App.l Phys*. **95**, 2690 (2004).